AJDR
Avicenna Journal of Dental Research
Avicenna J Dent Res, 2022; 14(3):113-119. doi:10.34172/ajdr.2022.21
http://ajdr.umsha.ac.ir

Original Article

The Effect of Gamma Values in Detection of Internal Root Resorption in CBCT Images: An *In Vitro* Study

Ali Habibi Kia[1], Mohsen Khataminia[2], Masoome Khataminia[3*]

[1]Assistant Professor, Department of Oral and Maxillofacial Radiology, Faculty of Dentistry, Ahvaz Jundishapur University of Medical Sciences, Ahvaz, Iran
[2]Undergraduate Dental Students, Department of Oral and Maxillofacial Radiology, Faculty of Dentistry, Ahvaz Jundishapur University of Medical Sciences, Ahvaz, Iran
[3]Assistant Professor, Department of Pediatric Dentistry, Faculty of Dentistry, Ahvaz Jundishapur University of Medical Sciences, Ahvaz, Iran

Article history:
Received: April 18, 2021
Received: November 3, 2021
ePublished: September 8, 2022

***Corresponding author:**
Masoome Khataminia, Assistant Professor, Department of Pediatric Dentistry, Faculty of Dentistry, Ahvaz Jundishapur University of Medical Sciences, Ahvaz, Iran.
Tel: +989166188429;
Email: khataminia-m@ajums.ac.ir

Abstract

Background: Accurate and early diagnosis of internal root resorption is essential for determining the outcome of treatment and prognosis. Several digital processing algorithms have been introduced for the diagnosis of internal root resorption. The aim of the present study was to evaluate the effect of gamma values in the detection of internal root resorption in cone-beam computed tomography (CBCT) images.

Methods: A total of 45 healthy extracted single-rooted teeth were selected for the study. The teeth were mesiodistally sectioned at the central groove of their occlusal surface using a diamond disc (0.1 mm diameter). Internal root resorption was simulated at the cervical, middle, and apical regions of a root canal. CBCT images were prepared by gamma values (low, medium, and high modes). Data were analyzed using McNemar tests, Cohen's kappa coefficient, and the receiver operating characteristic curve. A *P* value less than 0.05 (typically ≤ 0.05) was considered statistically significant.

Results: Sensitivity and overall accuracy of CBCT images with all gamma modes (low, medium, and high) were high, and they were slightly higher in the high gamma mode (Sensitivity: 94% and overall accuracy: 100%) than in two gamma modes (low and medium). The sensitivity and specificity of high and medium gamma modes in three regions of the root canal (cervical, middle, and apical) were at optimal thresholds compared to the low gamma mode.

Conclusions: Gamma modes, particularly the high gamma mode, in CBCT imaging can be adopted as a promising processing filter for the detection of internal root resorption.

Keywords: Gamma value, Internal root resorption, CBCT, Image processing

Please cite this article as follows: Habibi Kia A, Khataminia M, Khataminia M. The effect of gamma values in detection of internal root resorption in cbct images: an *in vitro* study. Avicenna J Dent Res. 2022; 14(3): 113-119. doi:10.34172/ajdr.2022.21

Background

Traumatic injuries are more common among the permanent anterior teeth and affect the adjacent bone and soft tissue. The most likely stimulation factors of root resorption are trauma or chronic pulpal inflammation. The exact mechanism of internal tooth resorption is not fully understood yet (1). Accurate and early diagnosis of internal root resorption is critical for determining the outcome of treatment and prognosis. A failure for early diagnosis of internal root resorption will lead to the progression of the lesion, weakening of the teeth structure, and poor long-term prognosis (2-4). In the radiographic feature, the resorptive lesion appears as a uniform, round-to-oval radiolucent enlargement of the pulp chamber (5).

Conventional periapical radiography and digital intraoral periapical radiography are the most commonly used techniques for the detection and analysis of internal root resorption (6-9). One of the major problems with the diagnosis of internal root resorption is the limited diagnostic information provided by intraoral radiography (6). These limitations are due to the two-dimensional (2D) nature of images, geometric distortion, and superimposition of structures (6). The diagnostic value of intraoral periapical radiography also depends on the extension and localization of the periapical lesion, and the diagnosis of small areas of periapical lesions is often difficult by intraoral periapical radiography (6-8). Some studies have shown that cone-beam computed tomography (CBCT) imaging provides more reliable images of the resorption area (internal/external), lesion location (cervical, middle, and apical), and size and proximity to root canal or periodontal space (6,10). Various data exist on the comparison of the accuracy of CBCT with conventional intraoral radiographs. The results indicated

that despite the diagnostic value of periapical radiography in detecting endodontic lesions, CBCT provides 3D images that display a true shape of internal root resorption. Thus, there is adequate reason to confirm that CBCT is an important source for early detection and appropriate diagnosis and treatment planning compared to periapical radiography (11-14).

Digital imaging systems provide a wide variety of image processing techniques with an extremely wider range of algorithms applied to the input data and avoid problems such as the build-up of noise and distortion during processing happening in the analog and other methods of imaging. The main purpose of signal/ image processing is to amplify diagnostic signals and eliminate the undesired signals or interferences. Software packages offer various filters for image processing, including inverse contrast, noise reduction, magnification, edge enhancement, smoothing, sharpening, and gamma value (6). Common graphics software allows setting the gamma correction value. For instance, gamma correction controls the overall brightness of an image (15).

Considering the important role of the early detection of internal root resorption in prognosis and treatment plan, as well as the limitations of intraoral techniques in the early detection of these lesions and insufficient studies on the effect of gamma changes in CBCT images, the present study examined the effect of gamma values in the detection of internal root resorption in CBCT images.

Materials and Methods

The present *in vitro* experimental study was conducted in Ahvaz Jundishapur University of Medical Sciences (AJUMS), Faculty of Dentistry. In general, 45 healthy single-rooted teeth extracted due to periodontal disease were selected for the study. The teeth were collected from dental offices in Ahvaz, in the southwest of Iran. The extracted teeth were sterilized by chlorhexidine 9% for 30 seconds, cleaned, and then stored in normal saline at room temperature. The inclusion criterion was teeth with no apparent caries, restoration, or fractures. The teeth were clinically healthy without a history of previous decay or restoration. The criterion for sample size computation was determined by previously validated studies (14).

Tooth Sectioning

The teeth were mesiodistally sectioned at the central groove of their occlusal surface using a diamond disc (0.1 mm diameter). Overall, 45 single-rooted teeth were mesiodistally split along the coronal plane into labial and lingual sections. The CBCT images were obtained before and after the formation of internal root resorption.

CBCT Preparation Before the Formation of Internal Root Resorption

In the first step, CBCT images were produced by connecting two halves of each tooth using the adhesive wax. Afterward, the samples were randomly divided into three equal anatomic and histologic landmarks of the root region (n = 15). The teeth from each group were mounted in a customized mold. To simulate bone density, the teeth were mounted in a mold with equivalent portions of plaster and acrylic powder (11). The surfaces of the samples were homogeneously smoothed by a model trimmer (Y-230; Yoshida, Tokyo, Japan). After mounting the teeth, to determine the position and establish a specific order in the numbering of the teeth, one side of each mold was marked with gutta-percha (radiopaque material). The mounted teeth were encoded, and the starting point of numbering in each mold was determined from the gutta-percha symbol.

CBCT images were prepared in the axial plane using the CBCT machine (NewTom, Giano, Verona, Italy), and cross-sectional CBCT images were prepared for each tooth (Figure 1). The scan parameters were set as mA = 3, kVp = 90, T = 9 ms, and FOV = 11 × 8 mm^2 kVp. An 11 × 15 cm CMOS-based detector was developed, and the images were saved as DICOM files. Then, the CBCT images were processed by NNT Viewer software (QR s.r.l., Verona, Italy) with image enhancement of the gamma value (Low = -30, medium = 0, and high = + 30). The section thickness of images was reconstructed at slice thickness = 0.5 mm and step = 0.5 mm. All the prepared images were labeled and registered accordingly (14).

CBCT Preparation After the Formation of Internal Root Resorption

In this phase, the teeth were separated into two halves. Internal root resorption with 1 mm wall thickness was simulated at the cervical of the labial wall using a high-speed handpiece with round diamond bur (1×1 mm; Tees Kavan Company, Tehran, Iran). Defects were prepared in the cervical (mold No. 1), middle (mold No. 2), and apical (mold No. 3) thirds. The sections were rejoined by super glue with similar thickness, compared with the adhesive wax used in the control group, and mounted in the mold in the previous position. CBCT images were obtained with the same scanning conditions (mA = 3, kVp = 90, T = 9, FOV = 11 × 8 kVp, Figure 2).

CBCT Image Evaluation

Two experienced radiologists, who were blind to the study, independently assessed the CBCT images in two sessions. A total of 270 CBCT images were evaluated on a 19-inch LED monitor (ASUS) with a resolution of 1024×1028 and 32 bits in a windowless dimly lit room. The images were coded with a numeric sign. The absence or presence of resorption lesions were blindly evaluated and reported by the two observers.

Data Analysis

The data obtained were interpreted and analyzed statistically using descriptive and analytical analysis, McNemar's significance test, Cohen's kappa coefficient, and SPSS, version 22 (SPSS Inc., Chicago, Ill., USA).

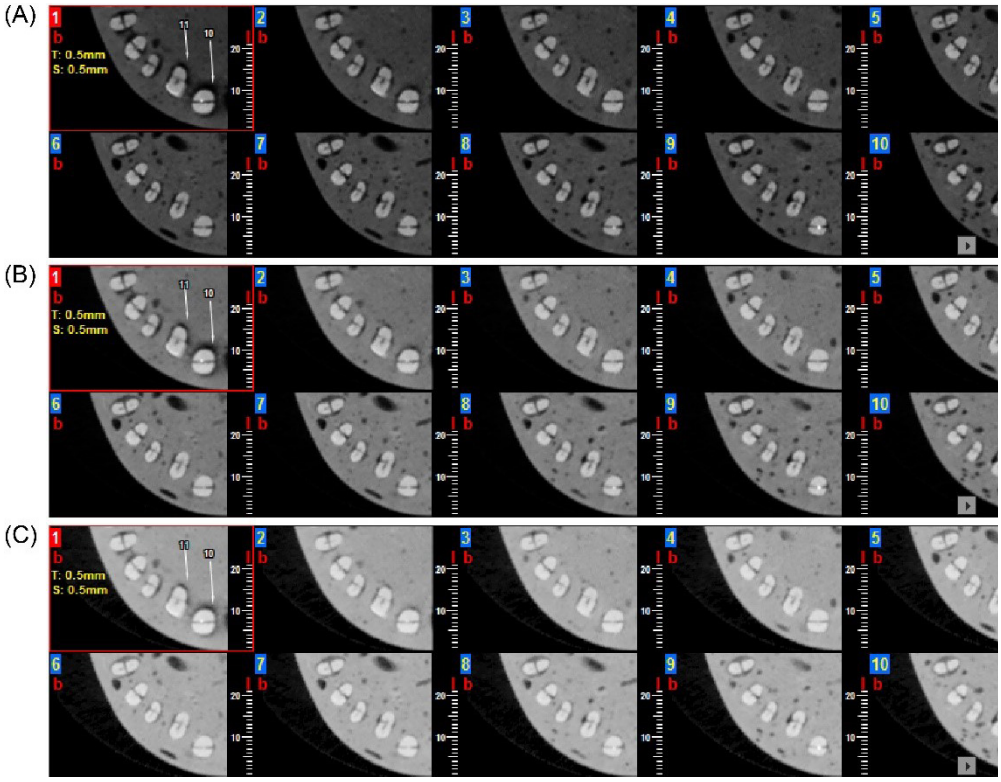

Figure 1. An Axial Section of CBCT in the Control Group: (A) High Gamma Mode, (B) Medium Gamma Mode, and (C) Low Gamma Mode. *Note*. CBCT: Cone-beam computed tomography.

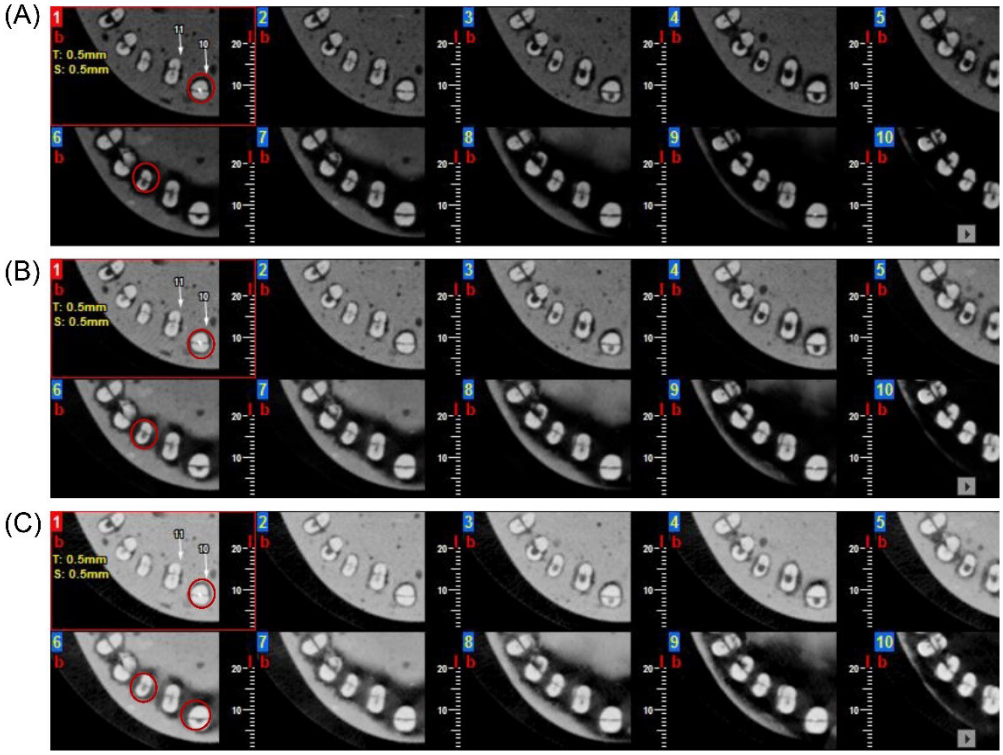

Figure 2. An Axial Section of CBCT in the Study Group: (A) High Gamma Mode, (B) Medium Gamma Mode, and (C) Low Gamma Mode. *Note*. CBCT: Cone-beam computed tomography. Some of the internal resorptions are marked with red circles.

Sensitivity, specificity, overall accuracy, positive predictive value, and negative predictive value were calculated, and a *P*-value less than 0.05 (typically ≤ 0.05) was considered statistically significant.

The CBCT images of teeth with and without resorption defects at different axial view levels (cervical, middle, and apical) were evaluated using three gamma value modes (Low, medium, and high). The Kappa value (inter-observer agreement) between the observers was assessed accordingly. Sensitivity and specificity were calculated,

and overall accuracy was computed with the ROC curve analysis.

The statistical analysis of low, medium, and high gamma images by the first observer is provided in Tables 1, 2, and 3. The agreement between the first and second observers in the low, medium, and high gamma modes was 0.599, 0.570, and 0.789.

The Area Under the ROC Curve (AUC) Analysis

The AUC values of the first observer regarding low, medium, and high gamma images were 77%, 82%, and 96%, respectively. There was no statistically significant difference between AUC values in low and medium modes in the first observer's viewpoint ($P>0.05$), but there was a statistically significant difference between AUC values in medium and high gamma modes ($P<0.05$). The AUC values of the second observer with respect to low, medium, and high gamma images were 88%, 93%, and 94%, respectively. Based on the results, no statistically significant difference was found between AUC values in three modes of the gamma value (low, medium, and high) in the second observer's point of view ($P>0.05$).

The results showed that the sensitivity and specificity regarding the high gamma mode were higher than those of low and medium gamma modes for the first observer, and for the second observer, the sensitivity in images with high and medium gamma modes was higher than that of the low gamma mode, and specificity in low and medium gamma modes was higher compared to the high gamma mode. The overall accuracy in the high gamma mode for the first observer was higher in comparison to low and medium gamma modes. There was a significant difference between the overall accuracy in the three modes of the gamma value (low, medium, and high). For the second observer, the overall accuracy was high in all modes of the gamma value and slightly higher in the high gamma mode. No significant difference was found between the overall accuracy of the three modes of the gamma value.

Based on the statistical analysis of the coronal area with low gamma images the sensitivity, specificity, and overall accuracy were 73.33%, 60%, and 67%, as well as 46.67%, 100%, and 73% for the first and second observers, respectively. The results of the McNemar test demonstrated a statistically significant difference between the imaging method with the low-gamma value and the standard-dose mode in the coronal area ($P<0.05$).

The obtained data on the middle area with low-gamma images by the first and second observers showed that the sensitivity, specificity, and overall accuracy were 100%, 52.63%, and 76%, as well as 100%, 100%, and 100%, respectively. According to the results of the McNemar test, a statistically significant difference was observed between the imaging method with the low-gamma value and the standard-dose mode in the cervical area ($P<0.05$).

As regards the statistical analysis of the apical area with low-gamma images, the sensitivity, specificity, and overall accuracy were reported to be 75%, 100%, and 88% by the first and second observers, respectively. Based on the

Table 1. Sensitivity, Specificity, and Overall Accuracy Values of Images With Low Gamma Mode

	Sensitivity	Specificity	Positive Predictive Value	Negative Predictive Value	Area Under the ROC Curve
Observer 1	66% (51.23%, 78.79%)	%88 (75.69%, 95.47%)	84.62% (69.47%, 94.14%)	72.13% (59.17%, 82.85%)	77% (0.68, 0.85) $P<0.001$
Observer 2	%76 (61.38%, 86.94%)	%100 (92.89%, 100%)	%100 (90.75%, 100%)	80.65% (68.63%, 89.85%)	88% (0.80, 0.94) $P<0.001$

Note. ROC: Receiver operating characteristic. Numbers in the second row of each cell are confidence intervals.

Table 2. Sensitivity, Specificity, and Overall Accuracy Values of Images With Medium Gamma Mode

	Sensitivity	Specificity	Positive Predictive Value	Negative Predictive Value	Area Under the ROC Curve
Observer 1	%92 (80.77%, 97.78%)	%72 (57.51%, 83.77%)	76.67% (63.96%, 86.62%)	%90 (76.34%, 97.21%)	82% (0.73, 0.89) $P<0.001$
Observer 2	%94 (83.45%, 98.75%)	%92 (80.77%, 97.78%)	92.16% (81.12%, 97.82%)	93.88% (83.13%, 98.72%)	93% (0.86, 0.97) $P<0.001$

Note. ROC: Receiver operating characteristic. Numbers in the second row of each cell represent confidence intervals.

Table 3. Sensitivity, Specificity, and Overall Accuracy Values of Images With High Gamma Mode

	Sensitivity	Specificity	Positive Predictive Value	Negative predictive value (NPV)	Area under the ROC Curve (AUC)
Observer 1	100% (92.89%, 100%)	92% (90%, 99%)	92.59% (82.11%, 97.94%)	100% (92.29%, 100%)	96% (0.90, 0.99) $P<0.001$
Observer 2	%100 (92.89%, 100%)	%88 (75.69%, 95.47%)	89.29% (78.12%, 95.97%)	%100 (91.96%, 100%)	94% (0.87, 0.98) $P<0.001$

Note. Numbers in the second row of each cell demonstrate confidence intervals.

results of the McNemar test, no statistically significant difference was detected between the imaging method with the low-gamma value and the standard-dose mode in the apical area ($P>0.05$).

The findings related to the coronal area with medium-gamma images represented that the sensitivity, specificity, and overall accuracy were 100%, 66.67%, and 83%, as well as 80%, 73.33%, and 77% by the first and second observers, respectively. Based on the results of the McNemar test, there was no statistically significant difference between the imaging method with the medium-gamma value and the standard-dose mode in the coronal area ($P>0.05$).

Likewise, the results related to the statistical analysis of the middle area with medium-gamma images by the first and second observers revealed that the sensitivity, specificity, and overall accuracy were 100%, 73.68%, and 87%, as well as 100%, 100%, and 100%, respectively. The results of the McNemar test showed no statistically significant difference between the imaging method with the medium-gamma value and the standard-dose mode in the cervical area ($P>0.05$).

According to the reports of the first and second observers regarding the analysis of the apical area with medium-gamma images, the sensitivity, specificity, and overall accuracy were 75%, 75%, and 75%, as well as 100%, 100%, and 100%, respectively. The obtained data related to the McNemar test demonstrated no statistically significant difference between the imaging method with a medium-gamma value and the standard-dose mode in the apical area ($P>0.05$).

Moreover, the statistical analysis of the coronal area with low-gamma images by the first and second observers represented that the sensitivity, specificity, and overall accuracy were 100%, 100%, and 100%, as well as 100%, 86.67%, and 93%, respectively. Based on the results of the McNemar test, no statistically significant differences were observed between the imaging method with a low-gamma value and the standard-dose mode in the coronal area ($P>0.05$).

Additionally, the findings of the statistical analysis of the middle area with medium-gamma images by the first and second observers indicated that the sensitivity, specificity, and overall accuracy were 100%, 78.95%, and 89%, as well as 100%, 100%, and 100%, respectively. The results of the McNemar test showed no statistically significant difference between the imaging method with a medium-gamma value and the standard-dose mode in the cervical area ($P>0.05$).

Finally, the data on the statistical analysis of the apical area with high-gamma images demonstrated 100%, 100%, and 100%, as well as 100%, 75%, and 88% for the sensitivity, specificity, and overall accuracy by the first and second observers, respectively. Based on the results of the McNemar test, there was no statistically significant difference between the imaging method with a high-gamma value and the standard-dose mode in the apical area ($P>0.05$).

Discussion

Radiology is a useful diagnostic tool for the detection of the abnormalities of skeletal and soft tissues and optimizes appropriate treatment by providing more accurate diagnostic planning parameters. Basically, any diagnostic method for internal root resorption must have the correct diagnostic ability (16). Internal root resorption is an inflammatory development originated within the pulp space with the loss of dentin and probable invasion of the cementum. The diagnosis of internal root resorption is difficult to establish and conventional X-ray radiography is often inadequate in this regard. CBCT is the most powerful imaging technique for the early and accurate diagnosis of resorptive lesions (17).

Advances in direct digital radiography led to the development of image processing and image quality control techniques. Digital image processing allows image enhancement by applying specific filters to detect carious lesions. These filters facilitate the analysis and interpretation of digital dental radiographs. However, the diagnostic value of the enhancement tools of digital imaging software is controversial (18,19).

Gamma correction or gamma value is a nonlinear process that is used in digital radiography to encode and decode luminance or tristimulus values in image systems. This technique has many image enhancement applications and can enhance a particular range of intensity levels. In digital radiography, altering the input signal by the gamma value increases the contrast value (the separation of the lightest and darkest parts of an image). In other words, increased gamma value input will result in increased brightness in all areas and increased contrast in the lower density region, while decreased gamma value input will lead to decreased brightness in all areas and increased contrast in the higher density region. Long scale contrast or low contrast is referred to as a radiograph that has a less noticeable density difference, but possesses many more shades of grey (15).

Several studies have examined the performance of CBCT images using different voxel sizes and filters for the detection of external and internal root resorption (20-23). The present study investigated the effect of gamma value changes in the detection of internal root resorption in single-rooted teeth. In the current study, the sensitivity and specificity regarding the high-gamma mode were higher than those of the other two modes (low and medium) according to the first observer. Further, for the second observer, the sensitivity in the images with high- and medium-gamma modes was higher compared to the low-gamma mode, and specificity in low- and medium-gamma modes was higher in comparison with the high-gamma mode. The overall accuracy in the high-gamma mode was higher than the overall accuracy of low- and medium-gamma modes for the first observer. A significant difference was found in the overall accuracy of three gamma modes (low, medium, and high). For the second observer, the overall accuracy was high in all (particularly

the high-gamma mode) gamma modes, and no significant difference was observed between the overall accuracy of the three modes of the gamma value (low, medium, and high). Therefore, the overall accuracy of the gamma value for both observers in the high-gamma mode was higher compared to the other two modes (low and medium).

Habibi Kia et al examined the efficacy of the gamma value for the detection of tooth-induced external root resorption, namely, the apical portion of single-root teeth in CBCT and concluded that the high-gamma mode had higher sensitivity and overall accuracy in comparison with low- and medium-gamma modes (19), which is consistent with the results of the present study.

In another study, the above-mentioned researchers evaluated the efficacy of gamma-value changes on the detection of proximal recurrent caries in a digital bitewing radiograph. The results of the study showed that the highest sensitivity and specificity values were related to the images with low- and medium-gamma images, respectively, while the lowest sensitivity and specificity values belonged to the images with a high-gamma mode (24), which contradicts the results of the present study. The reason could be differences in the density of amalgam materials used in the above-mentioned study (high density) and the present study (low density). Low gamma, in addition to reducing brightness, increases the contrast in the higher density region and leads to better detection of proximal recurrent caries with high density. Additionally, the high-gamma mode due to increased brightness and better contrast in darker areas increases the detection of proximal recurrent caries with low density.

In the present study, the alternation of gamma modes in the axial view of the CBCT image (cervical, middle, and apical) was also evaluated for more detail. The results revealed that the total sensitivity and specificity in the coronal region, using the high-gamma mode, was slightly better compared to medium- and low-gamma modes for both observers. Likewise, the sensitivity and specificity of all gamma modes in the cervical area were 100% for the first observer, but they were optimal in the high-gamma mode for the second observer. Similarly, the sensitivity and specificity in the apical area for the first and second observers were optimal in the high- and medium-gamma modes, respectively. Therefore, medium- and high-gamma modes can be widely applied in the diagnosis of internal root resorption involving the cervical, middle, and apical regions of the root canal.

Strengths and Limitations of the Study

The findings of this study have to be considered in light of some limitations. One of the limitations of this study was the artificial creation of a cavity with a round shape and with certain limits by round bur, which was not a completely characterized example of physiological resorption. Additionally, the depth of the cavities was the same in all cervical, middle, and apical areas. Moreover, due to the nature of the *in vitro* study, anatomical superimposition was unavailable. On the other hand, one of the valuable aspects of this research was the application of different degrees of gamma modes in NNT software for the diagnosis of internal root resorption.

Conclusions

Gamma modes, particularly the high-gamma mode, in CBCT imaging can be adopted as a promising processing filter for the detection of internal root resorption. The sensitivity and specificity of high- and medium-gamma modes in three regions of a root canal (cervical, middle, and apical) were at optimal thresholds compared to the low-gamma mode.

Acknowledgments

The authors would like to express sincere gratitude to the Vice-chancellor for Research and Technology, Ahvaz Jundishapur University of Medical Sciences (AJUMS) for the technical and financial support for this study.

Authors' Contribution

AHK, MoK, and MaK designed and performed experiments, analyzed data, and co-wrote the paper. AHK and MoK performed the experiments. AHK and MaK performed statistical analyses. AHK supervised the research.

Conflict of Interest Disclosures

The authors declare no conflict of interests.

Ethical Statement

The study was approved by the Ethics Committee of AJUMS (Registration No: IR.AJUMS.REC.1398.608).

References

1. Lyroudia KM, Dourou VI, Pantelidou OC, Labrianidis T, Pitas IK. Internal root resorption studied by radiography, stereomicroscope, scanning electron microscope and computerized 3D reconstructive method. Dent Traumatol. 2002;18(3):148-52. doi: 10.1034/j.1600-9657.2002.00012.x.
2. Kamburoğlu K, Kursun S. A comparison of the diagnostic accuracy of CBCT images of different voxel resolutions used to detect simulated small internal resorption cavities. Int Endod J. 2010;43(9):798-807. doi: 10.1111/j.1365-2591.2010.01749.x.
3. Glendor U, Marcenes W, Andreasen JO. Classification, epidemiology and etiology. In: Textbook and Color Atlas of Traumatic Injuries to the Teeth. 4th ed. John Wiley & Sons; 2007. p. 217-54.
4. Haapasalo M, Endal U. Internal inflammatory root resorption: the unknown resorption of the tooth. Endod Topics. 2006;14(1):60-79. doi: 10.1111/j.1601-1546.2008.00226.x.
5. Sigurdsson A, Trope MA, Civian N. The role of endodontics after dental traumatic injuries. In: Pathways of the Pulp. Mosby; 2011. p. 620-49.
6. Patel S. New dimensions in endodontic imaging: part 2. Cone beam computed tomography. Int Endod J. 2009;42(6):463-75. doi: 10.1111/j.1365-2591.2008.01531.x.
7. Kamburoğlu K, Barenboim SF, Kaffe I. Comparison of conventional film with different digital and digitally filtered images in the detection of simulated internal resorption cavities--an ex vivo study in human cadaver jaws. Oral Surg Oral Med Oral Pathol Oral Radiol Endod. 2008;105(6):790-7. doi: 10.1016/j.tripleo.2007.05.030.
8. Khalilak Z, Dadresanfar B, Mehralizadeh S, Fallahdoost A, Mokhberi L. Comparison of the diagnostic quality of the

conventional and digital radiography in detection of external root resorption cavities (invitro). J Res Dent Sci. 2012;8(4):194-9. [Persian].
9. Patel S, Dawood A, Whaites E, Pitt Ford T. New dimensions in endodontic imaging: part 1. Conventional and alternative radiographic systems. Int Endod J. 2009;42(6):447-62. doi: 10.1111/j.1365-2591.2008.01530.x.
10. Kiarudi AH, Eghbal MJ, Safi Y, Aghdasi MM, Fazlyab M. The applications of cone-beam computed tomography in endodontics: a review of literature. Iran Endod J. 2015;10(1):16-25.
11. Sharifi S, Maserat V, Safar Far A, Shah Siah S, Kavosi MA, Pur Mehdi M, et al. Comparison of diagnostic accuracy of cone beam computed tomography (CBCT) images and periapical radiograghy in internal root resorption lesions. Jundishapur Sci Med J. 2013;12(3):253-61. [Persian].
12. Madani Z, Moudi E, Bijani A, Mahmoudi E. Diagnostic accuracy of cone-beam computed tomography and periapical radiography in internal root resorption. Iran Endod J. 2016;11(1):51-6. doi: 10.7508/iej.2016.01.010.
13. Scarfe WC, Levin MD, Gane D, Farman AG. Use of cone beam computed tomography in endodontics. Int J Dent. 2009;2009:634567. doi: 10.1155/2009/634567.
14. Mehralizadeh S, Talayi Poor A, Mehrvarzfar P, Edalat M, Sharifi Shoushtari S. Comparison between digital intraoral radiography (PSP) and cone-beam CT images in detection internal root resorption (in-vitro study). J Res Dent Sci. 2016;13(2):102-8. [Persian].
15. White SC, Pharoah MJ. Oral Radiology-E-Book: Principles and Interpretation. Elsevier Health Sciences; 2014.
16. Nilsson E, Bonte E, Bayet F, Lasfargues JJ. Management of internal root resorption on permanent teeth. Int J Dent. 2013;2013:929486. doi: 10.1155/2013/929486.
17. Mehralizadeh S, Mehrvarzfar P, Taghizadeh S, Edalat M, Mohebi M. Reverse contrast enhancement in digital radiography in detection of vertical root fracture (in vitro). Journal of Dental Medicine. 2015;28(2):115-21. [Persian].
18. Farhadi N, Shokraneh A, Saatchi M. Effect of different levels of sharpness processing filter on the measurement accuracy of endodontic file length. Dent Hypotheses. 2016;7(1):15-9. doi: 10.4103/2155-8213.177408.
19. Habibi kia A, Khajavi G, Dabaghi A, Sharifi S, Esmaeili M, Haghighizadeh MH. Evaluation of the efficacy of gamma value changes on detection of proximal recurrent caries in digital bitewing radiograph. Jundishapur Scientific Medical Journal. 2021;19(6):545-54.
20. Liedke GS, da Silveira HE, da Silveira HL, Dutra V, de Figueiredo JA. Influence of voxel size in the diagnostic ability of cone beam tomography to evaluate simulated external root resorption. J Endod. 2009;35(2):233-5. doi: 10.1016/j.joen.2008.11.005.
21. de Azevedo Vaz SL, Vasconcelos TV, Neves FS, de Freitas DQ, Haiter-Neto F. Influence of cone-beam computed tomography enhancement filters on diagnosis of simulated external root resorption. J Endod. 2012;38(3):305-8. doi: 10.1016/j.joen.2011.10.012.
22. Neves FS, de Freitas DQ, Campos PS, de Almeida SM, Haiter-Neto F. In vitro comparison of cone beam computed tomography with different voxel sizes for detection of simulated external root resorption. J Oral Sci. 2012;54(3):219-25. doi: 10.2334/josnusd.54.219.
23. Habibi Kia A, Khajavi G, Dabaghi A, Sharifi S, Esmaeili M, Haghighizadeh MH. Evaluation of the efficacy of gamma value changes on detection of proximal recurrent caries in digital bitewing radiograph. Jundishapur Sci Med J. 2021;19(6):545-54. [Persian].
24. Russ JC, Russ JC. Introduction to Image Processing and Analysis. CRC Press; 2017.